Diagnosis of Insulated Building Walls Using Passive Infrared Thermography and Numerical Simulations

Jean-Pierre Monchau, Laurent Ibos, Vincent Feuillet

HAL Id: hal-01020325

https://inria.hal.science/hal-01020325

Submitted on 8 Jul 2014

Diagnosis of insulated building walls using passive infrared thermography and numerical simulations

Jean-Pierre Monchau[1], Laurent Ibos[1], Vincent Feuillet[1]

[1] *CERTES/OSU Efluve, Université Paris Est Créteil, 61 Avenue du Général de Gaulle, 94010 Créteil Cedex, France*

vincent.feuillet@u-pec.fr

Abstract

This work presents the thermal monitoring of a multi-layered wall of a restored building (PANISSE platform). Surface temperatures measured by infrared thermography are corrected by taking account of the influence parameters. Then they are compared with thermocouple measurements and numerical simulations.

Keywords : *building monitoring, passive infrared thermography, thermal modeling, thermal resistance.*

Introduction

Infrared thermography is frequently used for building monitoring because of several advantages. It is a non-intrusive measurement method that leads to high spatial and thermal resolutions. Despite that, infrared thermography is not commonly used for quantitative diagnosis because of the difficulty to understand in details all the influence parameters of the thermal scene to be viewed [1].

Currently there is only one international norm that defines an in-situ measurement method of the thermal resistance of insulated building walls based on the use of contact sensors (thermocouples and fluxmeters) [2]. However a new norm based on the use of infrared thermography is in preparation [3]. In literature, most studies involving passive infrared thermography in building monitoring leads to qualitative results. For example insulation defects are detected on building façades [4] or the influence of the measurement hour in the day is analyzed [5]. Only a few quantitative diagnoses by means of passive infrared thermography exist. A complete methodology based on the infrared thermovision technique has been developed to reach quantitative data of thermal transmittances of building envelopes [6]. However authors insist on the high influence of the measurement conditions (weather, managing of building by users, maintenance works, ageing of the building materials). Another interesting approach consists in investigating both visual and IR images in the same study [7] to yield a diagnosis of various façades with a significant reduction of the time analysis per evaluation.

In this study passive infrared thermography measurements on a multi-layered wall (PANISSE platform) are analysed. This building has been restored with an outside thermal insulation in 2011. A set of parameters is measured continuously: outside and inside air temperatures and humidities, surface wall temperatures. A fluxmetric method is used to measure the thermal resistance of the wall. Finally infrared temperature measurements are compared after correction with numerical simulation results.

1 Instrumentation and measurements

1.1 Description of the PANISSE platform

The PANISSE platform is a residential building with two floors located in the town of Villemomble, at about ten kilometres in the east of Paris. It was built in the sixties and walls are made of cellular concrete. During a renovation in 2011, a 6cm-thick external insulating layer was fixed onto eastern, northern and western façades. Southern wall is a shared with a symmetrical

house. Insulating material used is graphite expanded polystyrene. An air gap of about 1cm thick was kept between concrete wall and polystyrene layer. A schematic description of the wall structure is provided in Figure 1. The house is a lived-in home and its terrace roof is not thermally insulated. In the northern façade, a garage is used as a thermal guard (see Figure 2).
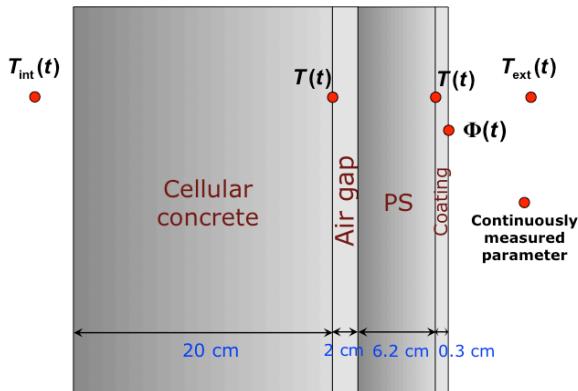

Figure 1: Schematic description of the PANISSE walls structure

A weather station was installed on the building roof. This device provides several parameters: wind direction and speed, air temperature, relative humidity, atmospheric pressure, rainfall amounts. During renovation works, K-type thermocouples were fixed onto several positions of the three free façades: 3 onto the eastern façade, 1 onto the northern façade and 6 onto the western façade (see Figure 2 for details). For each position, one thermocouple was fixed between the polystyrene and façade coating layers and another one was fixed onto the external face of the cellular concrete wall, as presented in Figure 1. Solar cells were fixed onto each of the free façades of the house and on the roof in order to measure the incident solar flux density on each façade. These solar cells were preliminarily calibrated by using a reference Kipp&Zonnen™ pyranometer. All sensors are connected to a National Instruments™ data acquisition device controlled by a LabView™ application. Data are recorded with a sampling period of 15 seconds since the beginning of 2013. Parameters values are stored in daily time stamped ASCII files.
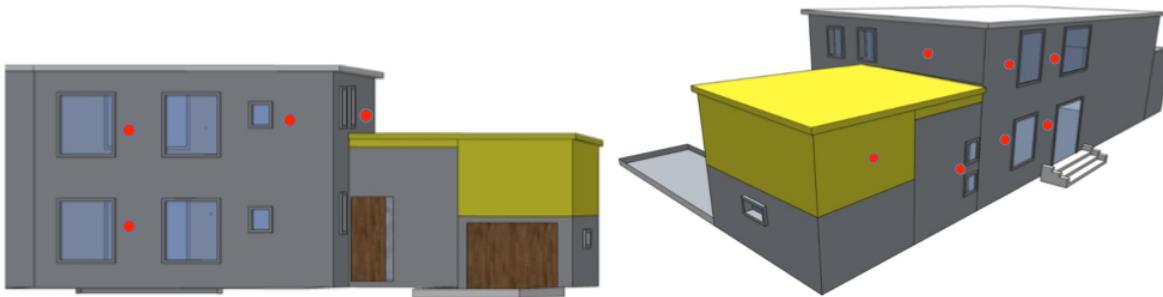

Figure 2: Views of the PANISSE platform; eastern and northern façades (left), northern and western façades (right); red points indicate the positions of thermocouples

Inside wall surface temperature is not measured. However, Warito™ data-loggers are used to record relative humidity and air temperature in several rooms of the house with a sampling period of 10 minutes. These data-loggers are provided with a calibration certificate: uncertainties on temperature and relative humidity are of 0.12°C and 3% respectively. Configuration and recorded data downloading is performed periodically through a USB interface.

Some preliminary measurements were performed to characterize optical properties of the coating used on each façade. The solar flux absorption coefficient was in-situ determined using a home-made albedometer. This device is composed of two opposite solar cells calibrated with a pyranometer. The ratio of both reflected and incident fluxes gives the albedo of the façade surface. The obtained value of absorption coefficient is $\alpha = 0.37$. In the same way, the emissivity of the façades coating was in-situ determined using a portable emissometer recently developed in the CERTES laboratory [8]. The emissivity value in the 8-14 μm band is $\varepsilon = 0.93$.

1.2 Infrared thermography measurement campaign

A measurement campaign by infrared thermography was performed in 2013 during 12 consecutive days between January 25 and February 6. The camera used is a FLIR™ SC 7300 LWIR camera (7.7-9.2 μm) with a Stirling cooled detector of 320 x 256 pixels. A standard 25 mm lens was used. Thus, the IFOV value is 1.3 mrad. The camera was connected through an Ethernet interface to a portable computer. Images were recorded each 15 seconds during 12 days using the Altair™ software. The infrared camera and computer were placed inside a watertight enclosure (see Figure 3). This enclosure was installed in the garden of the house in order to observe the western façade. An example of thermal image recorded during a sunny day is presented in Figure 3. Air temperature and relative humidity inside the enclosure were continuously monitored using a Warito™ data-logger.
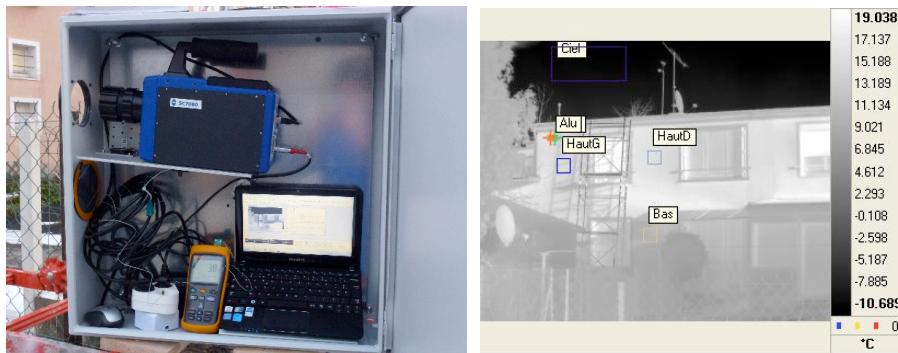

Figure 3: View of the thermographic instrumentation (left) and example of thermal image recorded during a sunny day (right)

A diffusive mirror of rough aluminium of 0.063 emissivity [9] and a black surface coated with a Nextel Velvet 811-21 coating of 0.97 emissivity were fixed on the upper left part of the investigated façade. Temperatures of both surfaces were recorded all along the measurement campaign using a numeric thermometer and two K-type thermocouples. The diffusive mirror allows computing the mean radiant temperature of the environment considered as a blackbody [9]. The black reference surface allows estimating the atmospheric attenuation.

Thermal image sequences are then corrected in order to take into account all parameters influencing computed values of the external wall surface temperature. These parameters are wall surface emissivity, mean radiant temperature, atmospheric transmission factor and atmospheric temperature [10]. An example of temperature variations recorded during the whole campaign by thermocouple and infrared camera is presented in Figure 4. These measurements concern the measurement zone in the left upper part of observed façade. The differences between infrared camera and thermocouple temperature measurements for three regions of the façade are plotted in Figure 5. Mean difference values obtained in that cases are -0.07°C, 0.15°C and 0.14°C respectively and corresponding standard deviations are 0.44°C, 0.43°C and 0.39°C. Thus, a satisfactory agreement between thermocouple and infrared camera measurements is obtained excepted for some cloudy and sunny alternating short periods.
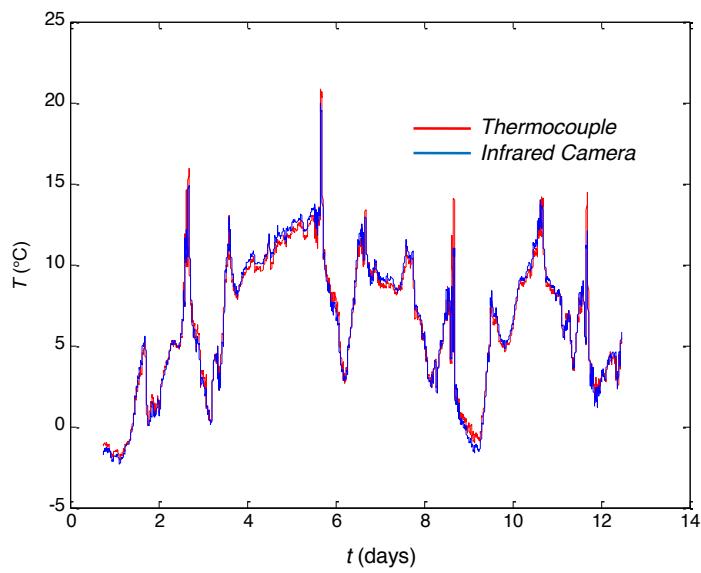
Figure 4: Comparison between thermocouple and corrected infrared measurements for the left upper zone of the western façade
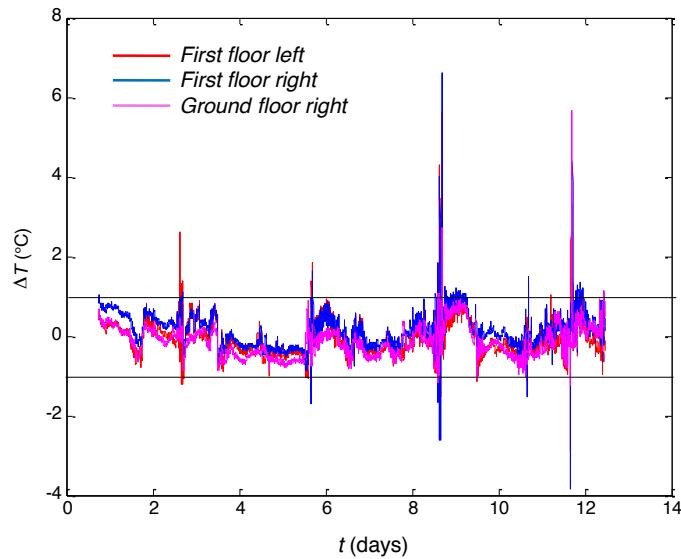

Figure 5: Temperature differences between thermocouple and corrected infrared measurements for three zones of the western façade

2   MEASUREMENT OF THE THERMAL RESISTANCE OF THE WALL

2.1   Principle

Two methods are used to measure the thermal resistance of the wall: the first one is based on the ISO-9869 norm [2], the second one uses the knowledge of the wall composition. The insulating layer is made of graphite expanded polystyrene that is 62 mm in thickness and 2 $m^2.K.W^{-1}$ in thermal resistance.

Figure 6 shows measurement points used. T_1 is the interior wall surface temperature, T_2 is the surface temperature between the cellular concrete and the air gap and T_3 is the exterior wall surface temperature. These measurements are done with K-type thermocouples. Interior and exterior air temperatures are measured with Warito™ sensors. HFM is a heat flux sensor from Captec™ (sensitivity 18 μV.W^{-1}.m^2).
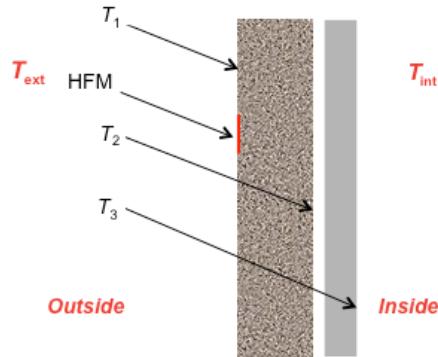

Figure 6: Schematic representation of the instrumentation used to measure the thermal resistance wall

2.2 Measurement with ISO-9869 norm

The measurement consists in computing time averages of the wall surface temperatures and of the heat flux. Time averages are ideally calculated on several days. One must check that accumulated energy in the wall is negligible compared to the energy transferred through the wall. A simple experimental approach is used: thermal resistance R_{th} is computed every 24h and the obtained value is confirmed if differences between two consecutive days are less than 5%. ISO-9869 describes a dynamic approach allowing taking account of the wall thermal inertia. The presented measurement lasted 48h. This could have been insufficient if meteorological conditions have not been suitable: cloudy sky, no sunshine, quite stable temperatures between day and night and equivalent conditions during the days before the measurement.

The total thermal resistance R_{th} is given as follows:

$$R_{th} = \frac{\langle T_1 \rangle - \langle T_3 \rangle}{\langle \Phi_S \rangle} \tag{1}$$

with Φ_s is the heat flux per unit surface area.

2.3 Method using the wall composition

The thermal resistance of the insulating layer is used to estimate the heat flux:

$$\langle \Phi_S \rangle = \frac{\langle T_2 \rangle - \langle T_3 \rangle}{R_{ins} + R_{gap}} \tag{2}$$

with R_{ins} is the thermal resistance of the insulating layer and R_{gap} the thermal resistance of the air gap. Then Φ_s is used to compute R_{th} with eq. (1).

2.4 Results

The average values of the two-day measurements are given in Table 1:

Table 1: Average value parameters to measure the thermal resistance of the wall

Average values of the two-day measurements					
T_{int} (°C)	T_1 (°C)	T_2 (°C)	T_3 (°C)	T_{ext} (°C)	Φ_S (W.m^{-2})
19.66	18.34	16.00	6.42	6.28	3.11

The computed heat flux with the second method gives Φ_s=3.46 W.m^{-2}. Thermal resistances obtained with the two methods are respectively: R_{th1}=3.83 m^2.K.W^{-1} et R_{th2}=3.44 m^2.K.W^{-1}. The difference between the two methods is about 10%, which is reasonable for a fluxmetric method.

3   COMPARISON BETWEEN MEASUREMENTS AND NUMERICAL SIMULATIONS

3.1   Principle

In this part measurements are compared with simulation results obtained with a modeling of the heat transfer in the wall. Analysis concerns the measurements on the first floor of the western façade. The numerical simulation is achieved with commercial software Comsol^{TM} that solves the studied thermal system thanks to the finite element method.

First the heat transfer modeling is described in terms of domains and boundary conditions. The different parameters of the modeling are also defined. The simulated wall is presented in Table 2 along with its geometrical and thermophysical properties. An air gap is put between the cellular concrete and the expanded polystyrene. Figure 7 presents a schematic description of the wall considered in the thermal modeling. The wall is submitted to heat exchanges both on interior and exterior surfaces, respectively with constant global heat transfer coefficients h_{int} and h_{ext} and air temperatures T_{int}(t) and T_{ext}(t). We consider mono dimensional heat transfer by conduction in the z-direction through the layers of the wall (thickness e_i, thermal conductivity λ_i, density ρ_i, heat capacity c_i). Solar heat flux Φ_0(t) is absorbed by the exterior wall surface by considering the absorption factor α of the surface alpha. The air gap is modeled by taking account of a thermal resistance R_{gap} between the concrete and the insulating layer. Indeed the investigation area is taken in the center of the wall, distant from windows and thermal bridges. Heat transfer parameters from literature [11] or measurement (coefficient α) are reported in Table 3.
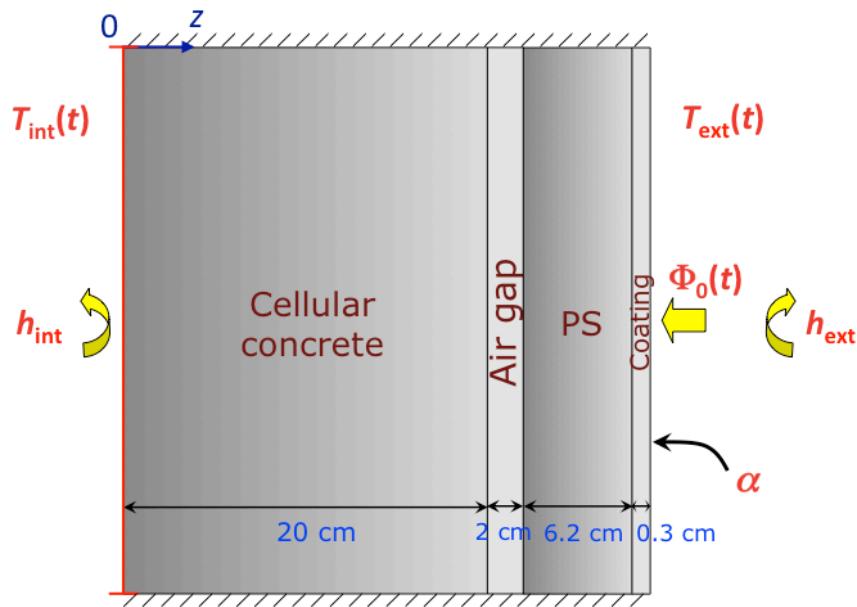

Figure 7: Schematic representation of the wall considered in the thermal modeling

Table 2: Geometrical and thermophysical properties of the wall studied in the modeling

Layer i	Thickness e_i (cm)	Thermal conductivity λ_i (W.m^{-1}.K^{-1})	Density ρ_i (kg.m^{-3})	Heat capacity c_i (J.K^{-1}.kg^{-1})
Cellular concrete (i=1)	20	0.14	400	1000
Expanded polystyrene (i=2)	6.2	0.031	20	1450
Coating (i=3)	0.3	0.3	833	1000

Table 3: Heat transfer parameters used in the modeling

h_{int} (W.m^{-2}.K^{-1})	h_{ext} (W.m^{-2}.K^{-1})	α	R_{gap} (m^2.K.W^{-1})
25	8	0.37	0.15

3.2 Results

The exterior wall surface temperature measured by IR thermography is compared with the temperature calculated with modeling presented in 3.1. The measured meteorological parameters are used in the modeling. The Figure 8(a) shows measured and calculated temperatures T_{mea} and T_{cal} for 7 days of measurement. The Figure 8(b) shows the corresponding differences T_{mea}-T_{cal}.

We note a correct similarity between measurement and modeling temperature profiles for the considered period. However a bias is observed along the investigated period, the measured temperature is globally inferior to the calculated temperature. The temperature difference average is -0.71°C while the standard deviation is 0.63°C. The most important discrepancies appear when rapid variations of the solar flux are observed. The next step of the study will consist in using a parameter estimation method to decrease these differences by adjusting some modeling parameters.
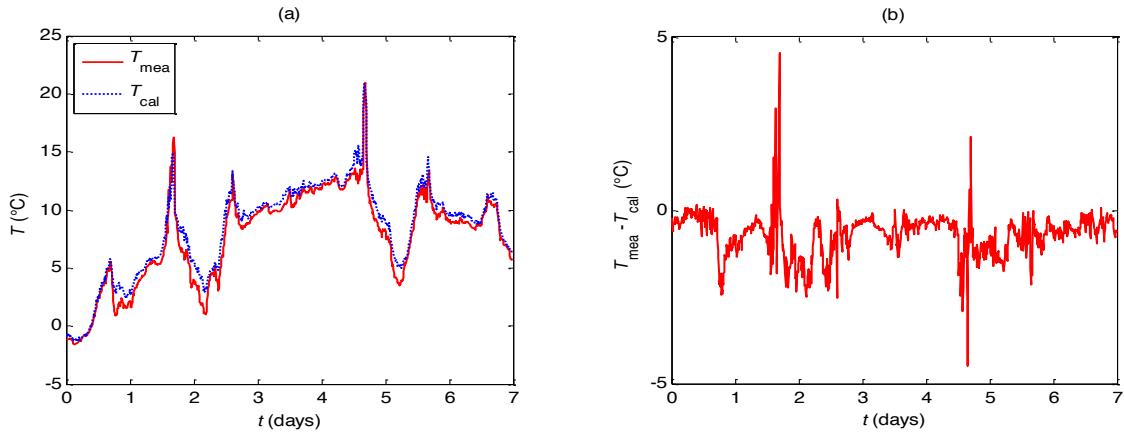

Figure 8: Exterior wall surface temperatures – first floor of the western façade
(a) Measured and calculated temperatures T_{mea} and T_{cal}, (b) Differences T_{mea}-T_{cal}

CONCLUSION

This work presents the instrumentation of a lived-in home allowing the thermal monitoring of the walls of the building. The first step of the study consists in correcting the wall surface temperatures measured by infrared thermography by taking account all the influence parameters (wall surface emissivity, mean radiant temperature, atmospheric transmission factor and atmospheric

temperature). The proposed correction method is evaluated by comparing with K-type thermocouple measurements. The following step shows a correct similarity between measured exterior wall surface temperatures and modeling results calculated with the finite elements method.

The next step will consist in estimating unknown parameters in the modeling in order to determine the thermal resistance of the wall. This value will be compared with the one obtained with the fluxmetric method. This identification is achieved by solving the corresponding inverse problem formulated in the least-squares sense. It consists in minimizing the functional that links the measured and calculated temperatures by using Levenberg-Marquardt algorithm [12].

REFERENCES

[1] E. Bareira, V. P. de Freitas. Evaluation of building materials using infrared thermography. *Construction and Building Materials*, 21:218–224, 2007.

[2] Norme ISO 9869-1, 1994.

[3] S. Kato, K. Kuroki, S. Hagihara. Method of in-situ measurement of thermal insulation performance of building elements using infrared camera. *6th International Conference on Indoor Air Quality, Ventilation & Energy Conservation in Buildings (IAQVEC)*, Sendai, Japon, October 2007.

[4] C. A. Balaras, A. A. Argiriou. Infrared thermography for building diagnostics. *Energy and Buildings*, 34:171–183, 2002.

[5] S. M. Ocaña, I. C. Guerrero, I. G. Requena, Thermographic survey of two rural buildings in Spain. *Energy and Buildings*, 36:515–523, 2004.

[6] R. Albatici, A. M. Tonelli. Infrared thermovision technique for the assessment of thermal transmittance value of opaque building elements on site. *Energy and Buildings*, 42:2177–2183, 2010.

[7] S. Ribarić, D. Marčetić, D. S. Vedrina. A knowledge-based system for the non-destructive diagnostics of façade isolation using the information fusion of visual and IR images. *Expert Systems with Applications*, 36:3812–3823, 2009.

[8] J.P. Monchau, M. Marchetti, L. Ibos, J. Dumoulin, V. Feuillet, Y. Candau. Infrared emissivity measurements of building and civil engineering materials. *International Journal of Thermophysics*, in press.

[9] S. Datcu, L. Ibos, Y. Candau, S. Matteï. Contribution to improvement of building wall surface temperature measurements by infrared thermography. *Infrared Physics and Technology* 46:451-467, 2005.

[10] J.P. Monchau. Mesure d'émissivité pour la thermographie infrarouge appliquée au diagnostic quantitatif des structures. *PhD Thesis*, *Université Paris-Est*, November 2013.

[11] Réglementation Thermique 2012 (in French). *Ed. Centre Scientifique et Technique du Bâtiment*, 2012.

[12] D. W. Marquardt. An algorithm for the least squares estimation of non linear parameters. *SIAM Journal*, 1:431–441, 1963.